

Heat treatment of ion-irradiated silica-based thin films

S.A. Shojae^a, Y. Qi^b, Y.Q. Wang^c, T. Prenz^d, A. Mehner^d, D.A. Lucca^{b,*}^a Amethyst Research Inc., 123 Case Circle, Ardmore, OK 73401, USA^b School of Mechanical and Aerospace Engineering, Oklahoma State University, Stillwater, OK 74078, USA^c Division of Materials Science and Technology, Los Alamos National Laboratory, Los Alamos, NM 87545, USA^d Leibniz-Institut für Werkstofforientierte Technologien, Badgasteiner Str. 3, 28359 Bremen, Germany

ARTICLE INFO

Keywords:

Raman spectroscopy
FT-IR spectroscopy
Sol-gel processing
Ion irradiation

ABSTRACT

The microstructural relaxation caused by heat treatment of ion-irradiated silica-based thin films was investigated. Hybrid organic-inorganic silica-based thin films were synthesized via a sol-gel process and were irradiated with 125 keV H⁺ or 250 keV N²⁺ ions with fluences of 10¹⁵ or 10¹⁶ ions/cm². Ion irradiation was followed by heat treatment at 1100 °C or 1350 °C in an inert Ar atmosphere. The microstructure of the irradiated films before and after heat treatment was studied with a combination of Raman and infrared spectroscopies. The results indicated that while ion irradiation led to a defective structure of silica and graphitic C nanodomains, subsequent heat treatment led to structural relaxation and atomic reconfiguration of both silica and C. After heat treatment at 1100 °C, the microstructure of the films consisted of nanocrystalline graphite and structurally relaxed silica. After secondary heat treatment at 1350 °C, most of the C within the films vanished and the film microstructure only consisted of α-cristobalite silica.

1. Introduction

Silicon oxycarbides (SiOC) have found use in a range of applications including thermoelectric materials [1], radiation-resistant barriers [2], and ceramic foams [3]. SiOC derived from organosilicon ingredients has been traditionally decomposed into its final ceramic state via heat treatment. Ion irradiation has also emerged as an alternative method to decompose the starting organic materials into a final inorganic phase [4–6]. Our previous studies on the formation of SiOC ceramic thin films have indicated that utilizing ion irradiation instead of heat treatment leads to the formation of films with higher elastic modulus and hardness [7]. The microstructure of the films created via ion irradiation is fundamentally different from the films created via heat treatment, including a higher level of disorder and defects. In some cases the microstructural defects caused by ion irradiation in silica resemble the effects of high pressure compression [8,9]. While there has been some limited studies on the effects of a secondary heat treatment on ion-irradiated films [10], to the best of our knowledge, there has not been a systematic study of the effects of secondary heat treatment on the microstructure of ion-irradiated SiOC thin films. This work aims at studying the effects of a secondary heat treatment after ion irradiation on the microstructure of these films.

2. Experimental

The thin films were synthesized from a mixture of methyltriethoxysilane (MTES) and tetraethylorthosilicate (TEOS) organosilicon precursors using NaOH as a catalyst. First, 0.4 mol TEOS and 0.6 mol MTES were mixed together and then 0.96 mol of NaOH was dissolved in the mixture. The solution was stored in a three-neck round bottom flask for 24 h under an Ar atmosphere. Then a mixture of 5.66 mol distilled water and 1 mol ethanol was added drop by drop to the solution while held at a constant temperature of 35 °C. The final solution was stored at room temperature for one day under an Ar atmosphere prior to deposition. The prepared sol was spin-coated onto polished (1 0 0) Si wafers. The coated wafers were then dried at 80 °C for 10 min, followed by a 30 min heat treatment at 300 °C.

Ion irradiation of the films was performed using either 125 keV H⁺ or 250 keV N²⁺ ions with fluences of 10¹⁵ or 10¹⁶ ions/cm². A secondary heat treatment was also performed on the ion-irradiated films at 1100 °C or 1350 °C in an inert Ar atmosphere for 2 h. In addition to the ion-irradiated films, an unirradiated film was also heat treated.

The FT-IR spectra of the films were collected in reflection mode using a commercially available FT-IR instrument and a mid-infrared emitter. Raman spectroscopy was performed using a confocal Raman microscope utilizing a 532 nm laser light source. The light was focused on the surface using a 100x/0.9NA objective and the scattered light was

* Corresponding author.

E-mail address: lucca@okstate.edu (D.A. Lucca).<https://doi.org/10.1016/j.nimb.2019.03.044>

Received 15 September 2018; Received in revised form 16 March 2019; Accepted 20 March 2019

0168-583X/© 2019 Elsevier B.V. All rights reserved.

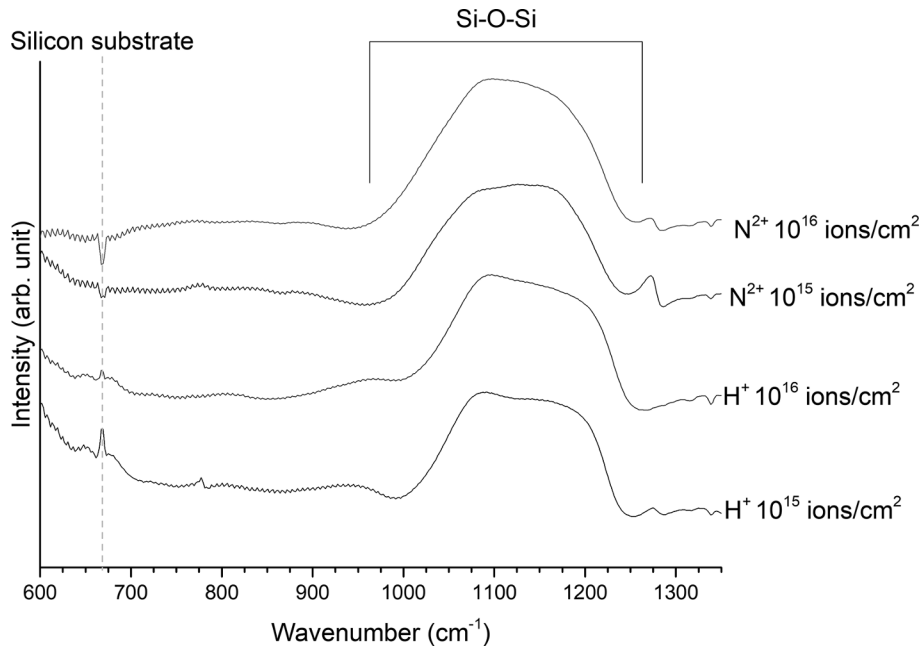


Fig. 1. FT-IR spectra of the films irradiated with different ion species and fluences.

collected using the same objective. The light was then focused on a confocal pinhole, a 100 μm diameter optical fiber, and was later dispersed by a 600 g/mm grating and detected by a thermoelectrically cooled CCD camera. XRD experiments were performed using a Cu-K α X-ray source and a Bruker D8 Discover diffractometer in the 2θ range of 10–60°.

3. Results and discussion

Fig. 1 shows the FT-IR response of the films irradiated with different ion species and fluences. In addition to the FT-IR peak around 670 cm^{-1} , which originates from the silicon substrate [11], the dominant peaks are related to the Si–O–Si bonds of silica. The main FT-IR peak of silica is the transverse optical (TO) peak, located at 1083 cm^{-1} for fused silica. In porous silica films, it is also possible to observe the longitudinal optical (LO) peak at around 1230 cm^{-1} [12]. In addition, the introduction of C into the silica structure gives rise to an additional peak around 1040 cm^{-1} [13,14]. As a result, the FT-IR response of C-containing silica is a broad peak between 1000 and 1250 cm^{-1} . The Si–O–Si bond angle can be estimated from the spectral center of the TO peak [15]. Based on curve fitting results, while some variations can be observed, the spectral center of all the films is within the 1070–1085 cm^{-1} range, corresponding to the bond angle range of 142–145°, which is in the expected range for the tetrahedrally bonded amorphous silica. We have previously reported on the effects of ion irradiation with H $^{+}$ and N $^{2+}$ ions on the Si–O–Si bond angle variation of similar silica based films [16].

Fig. 2 shows the Raman spectra of the films irradiated with N $^{2+}$ with fluences of 10 15 and 10 16 ions/cm 2 and also the H $^{+}$ -irradiated film with a fluence of 10 16 ions/cm 2 . The rest of the films exhibited C related peaks indicating the formation of free C clusters. Broadening of C related D and G modes because of the presence of defects, dangling bonds, and bond distortions leads to the appearance of a single asymmetric peak between 1200 and 1700 cm^{-1} . In order to investigate the nature of free C clusters in the films, curve fitting was performed using two Gaussian peaks for the D and G modes after a linear background subtraction, following a previously described method [17,18]. The intensity ratio of the D to G mode and the spectral center of the G mode can then be utilized to identify the nature of the free C clusters [17]. The curve fitting results indicate a G mode spectral center of

$\sim 1530 \text{ cm}^{-1}$ and a I(D)/I(G) ratio of ~ 1 for both N $^{2+}$ -irradiated films, which are indications of sp 2 -bonded and amorphous C with cluster sizes smaller than 20 Å. The size of such clusters can be estimated from [17]:

$$\frac{I(D)}{I(G)} = C'(\lambda)L_a^2 \quad (L_a \leq 20 \text{ Å}) \quad (1)$$

where C' is a constant related to the laser wavelength (λ), and L_a is the cluster size. For the laser wavelength of 532 nm used in this study, we have previously estimated C' to be 0.006 [16]. Based on this, the average C cluster size in both N $^{2+}$ -irradiated films was estimated to be 1.2 nm. The Raman response of the H $^{+}$ -irradiated film with a fluence of 10 16 ions/cm 2 had a higher signal to noise ratio, which made curve fitting not possible. In summary, the microstructure of the films after ion irradiation was deemed to be a combination of amorphous silica and sp 2 -bonded amorphous free C clusters.

Fig. 3 shows the FT-IR spectra of the films after secondary heat treatment at 1100 °C or 1350 °C. In addition to previously discussed FT-IR peaks, another FT-IR peak around 800 cm^{-1} can be observed which is related to Si–O–Si bonds [19,20]. The results indicate that after heat treatment the relative intensity of the LO peak compared to the TO peak has decreased, as evident from the smaller shoulder on the higher wavenumber side of the main Si–O–Si peak. The decrease is related to a reduction in the porosity of the films [12,21]. This is an expected effect of the secondary heat treatment, as sintering and densification occur at elevated temperatures. In addition, the spectral center of the TO peak has shifted to higher wavenumbers. The spectral centers of the TO peak in the FT-IR spectra of all the films are between 1094 and 1100 cm^{-1} , which corresponds to the bond angle of 149°, close to the bond angle of α -cristobalite [22]. This increase in the bond angle and the appearance of the α -cristobalite phase in the films after the secondary heat treatment is an indication of structural relaxation and atomic reconfiguration in the silica phase after secondary heat treatment.

Fig. 4 shows the Raman spectra of the irradiated films after secondary heat treatment at 1100 °C. None of the films heat treated at 1350 °C exhibited any C related Raman modes and therefore are not presented here. The loss of C after heat treatment at 1350 °C may explain the crystallization of the films heat treated at this temperature. The crystallinity of the films irradiated with N $^{2+}$ at a fluence of 10 16 ions/cm 2 after secondary heat treatment was studied using XRD.

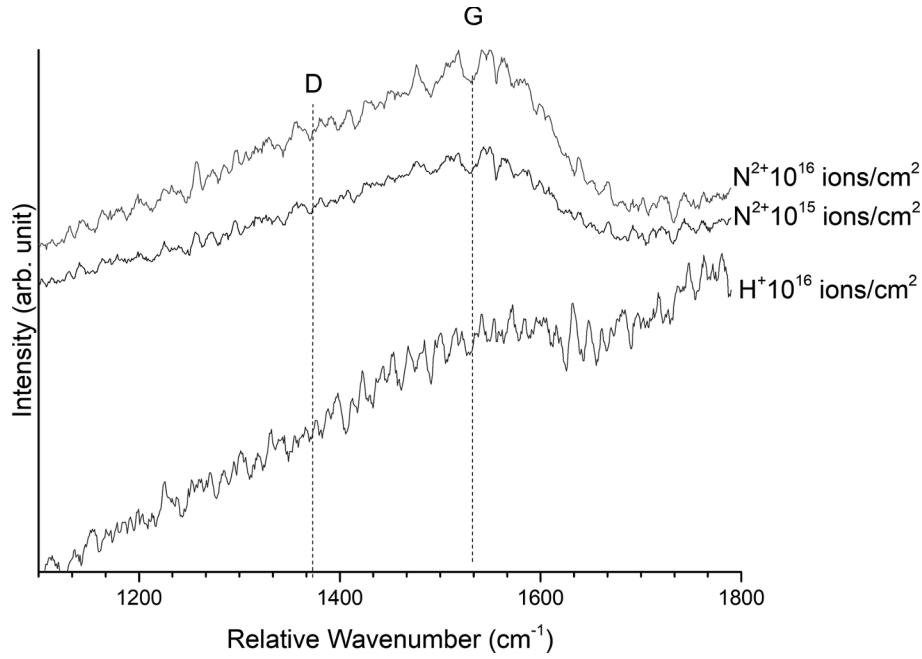


Fig. 2. Raman spectra of the ion-irradiated films that exhibited C related D and G modes.

Only the XRD pattern of the film heat treated at 1350 °C showed α -cristobalite peaks (JCPDS Number: 39-1425) and the XRD pattern of the film heat treated at 1100 °C only exhibited a broad amorphous silica peak (results not shown here). In SiOC materials developed from heat treatment alone, silica has been shown to stay amorphous up to 1500 °C, even though amorphous silica is known to crystallize to α -cristobalite at 1200 °C [23]. While many different explanations have been put forward to explain the resistance of SiOC to crystallization [24,25], all involve the role of C atoms. Therefore, C removal during secondary heat treatment may explain the crystallization of the silica in the film after 1350 °C heat treatment and crystallization may not be due to the effects of ion irradiation. Irradiation-induced crystallization has been observed in other material systems before [26,27], however, no such effect was observed in our SiOC films.

Curve fitting of the Raman response of the films after secondary heat treatment was achieved using two Breit-Wigner-Fano (BWF) lineshapes, which are more suitable than the Gaussian lineshape for more ordered C clusters. The Raman mode of all the films exhibited G modes centered around $\sim 1600 \text{ cm}^{-1}$ and $I(D)/I(G)$ ratios between 1 and 1.3, which are indications of nanocrystalline graphitic clusters with average sizes larger than 20 Å [17]. The size of such clusters can be estimated

from:

$$\frac{I(D)}{I(G)} = \frac{C(\lambda)}{L_a} \quad (L_a \geq 20 \text{ Å}) \quad (2)$$

where $C(\lambda)$ is a constant related to the laser wavelength (λ). We have calculated the constant value for the 532 nm laser as 50 Å before [16]. As a result, the C cluster sizes in all of the heat treated films, including the unirradiated film, were estimated to be between 4 and 5 nm, which is larger than the 1.2 nm size for that of the as-irradiated films. The amorphous C clusters in the present study were similar to C clusters in SiOC materials developed by heat treatment alone [28,29] in terms of crystallinity, sp-hybridization, and size. The results indicate that while the microstructure of the films after ion irradiation exhibits an atomic structure with a high concentration of defects, secondary heat treatment of ion-irradiated films leads to a structural relaxation and forms a structure that is similar, if not identical, to the films developed solely via heat treatment. The results indicate that the effects of ion irradiation on the microstructure of silica and carbon clusters, at these specific ion energies and fluences, can be removed.

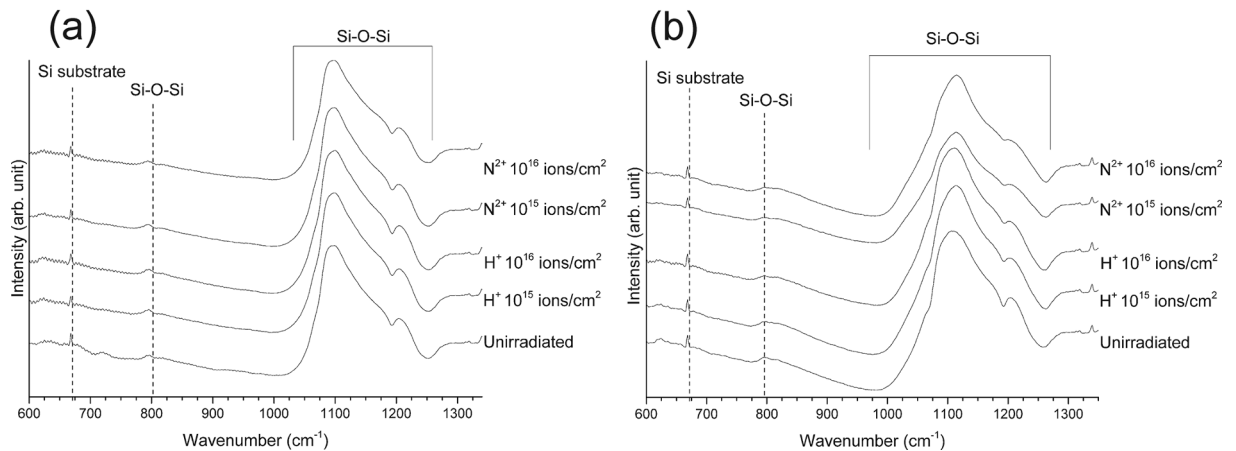


Fig. 3. FT-IR spectra of ion-irradiated films after secondary heat treatment at (a) 1100 °C and (b) 1350 °C.

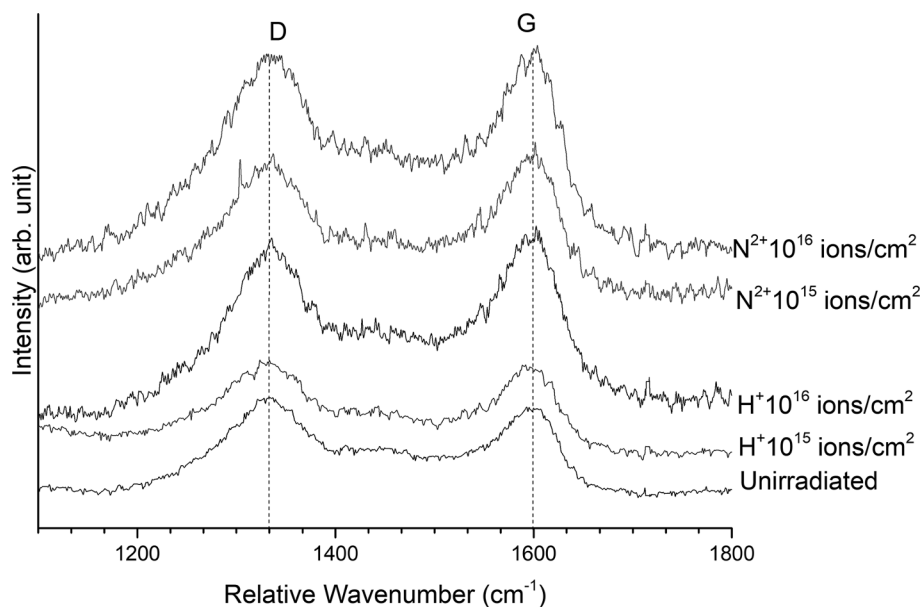


Fig. 4. Raman spectra of ion-irradiated films after secondary heat treatment at 1100 °C.

4. Conclusions

Silica based thin films irradiated with H^+ and N^{2+} were heat treated at elevated temperatures and the changes in their microstructures were studied using FT-IR and Raman spectroscopy. The results indicated that while the original microstructure after ion irradiation was disordered and contained defects, secondary heat treatment led to the formation of a reconfigured and relaxed microstructure. The results indicated that a secondary heat treatment can remove the irradiation-induced structural modifications.

Acknowledgements

The authors appreciate the financial support from the National Science Foundation (Grants Nos. OISE-0352377 and OISE-0128050). The authors are also grateful for the support from the Deutsche Forschungsgemeinschaft in Transregionaler Sonderforschungsbereich SFB/TR4. This work was performed, in part, at the Center for Integrated Nanotechnologies, an Office of Science User Facility operated for the U.S. Department of Energy (DOE) Office of Science by Los Alamos National Laboratory (Contract DE-AC52-06NA25396) and Sandia National Laboratories (Contract DE-NA-0003525).

References

- [1] A.B. Kousaalya, X. Zeng, M. Karakaya, T. Tritt, S. Pilla, A.M. Rao, Polymer-derived silicon oxycarbide ceramics as promising next-generation sustainable thermoelectrics, *ACS Appl. Mater. Interfaces* 10 (2018) 2236–2241.
- [2] A. Zare, Q. Su, J. Gigax, S.A. Shojaei, M. Nastasi, L. Shao, D.A. Lucca, Effects of ion irradiation on structural and mechanical properties of crystalline Fe/amorphous SiOC nanolaminates, *Acta Mater.* 140 (2017) 10–19.
- [3] P. Colombo, M. Modesti, Silicon Oxycarbide ceramic foams from a preceramic polymer, *J. Am. Ceram. Soc.* 82 (2004) 573–578.
- [4] V.K. Mittal, S. Lotha, D.K. Avasthi, Hydrogen loss under heavy ion irradiation in polymers, *Radiat. Eff. Defects Solids* 147 (1999) 199–209.
- [5] D.K. Avasthi, J.P. Singh, A. Biswas, S.K. Bose, Study on evolution of gases from Mylar under ion irradiation, *Nucl. Instrum. Methods B* 146 (1998) 504–508.
- [6] J. Pivin, P. Colombo, M. Sendova-Vassileva, J. Salomon, G. Sagon, A. Quaranta, Ion-induced conversion of polysiloxanes and polycarbosilanes into ceramics: Mechanisms and properties, *Nucl. Instrum. Methods B* 141 (1998) 652–662.
- [7] S.A. Shojaei, Y. Qi, Y. Wang, A. Mehner, D.A. Lucca, Ion irradiation induced structural modifications and increase in elastic modulus of silica based thin films, *Sci. Rep.* 7 (2017) 40100.
- [8] Q. An, L. Zheng, S.-N. Luo, Vacancy-induced densification of silica glass, *J. Non-Cryst. Solids* 352 (2006) 3320–3325.
- [9] L. Zheng, Q. An, R. Fu, S. Ni, S.-N. Luo, Densification of silica glass at ambient pressure, *J. Chem. Phys.* 125 (2006) 154511.
- [10] J.C. Pivin, P. Colombo, G.D. Soraru, Comparison of ion irradiation effects in silicon-based preceramic thin films, *J. Am. Ceram. Soc.* 83 (2000) 713–720.
- [11] P. Innocenzi, M.O. Abdirashid, M. Guglielmi, Structure and properties of sol-gel coatings from methyltriethoxysilane and tetraethoxysilane, *J. Sol-Gel Sci. Technol.* 3 (1994) 47–55.
- [12] P. Innocenzi, Infrared spectroscopy of sol-gel derived silica-based films: a spectro-microstructure overview, *J. Non-Cryst. Solids* 316 (2003) 309–319.
- [13] H.J. Lee, K.S. Oh, C.K. Choi, The mechanical properties of the SiOC(H) composite thin films with a low dielectric constant, *Surf. Coat. Technol.* 171 (2003) 296–301.
- [14] J. Kaspar, C. Terzioglu, E. Ionescu, M. Graczyk-Zajac, S. Hapis, H.-J. Kleebe, R. Riedel, Stable SiOC/Sn nanocomposite anodes for lithium-ion batteries with outstanding cycling stability, *Adv. Funct. Mater.* 24 (2014) 4097–4104.
- [15] A. Lehmann, L. Schumann, K. Hübner, Optical phonons in amorphous silicon oxides. I. calculation of the density of states and interpretation of LO-TO splittings of amorphous SiO_2 , *Phys. Status Solidi* 117 (1983) 689–698.
- [16] S.A. Shojaei, Y. Qi, Y.Q. Wang, A. Mehner, D.A. Lucca, Microstructural evolution of ion-irradiated sol-gel-derived thin films, *J. Mater. Sci.* 52 (2017) 12109–12120.
- [17] A. Ferrari, J. Robertson, Interpretation of Raman spectra of disordered and amorphous carbon, *Phys. Rev. B* 61 (2000) 14095–14107.
- [18] B. Marchon, J. Gui, K. Grannen, G.C. Rauch, J.W. Ager III, S.R.P. Silva, J. Robertson, Photoluminescence and Raman spectroscopy in hydrogenated carbon films, *IEEE Trans. Magn.* 33 (1997) 3148–3150.
- [19] G. Hasegawa (Ed.), *Studies on Porous Monolithic Materials Prepared via Sol-gel Processes*, Chapter: Fabrication of Macroporous SiC and SiC/C Monoliths from Arylene-bridged Polysilsesquioxanes via Carbothermal Reduction, Springer Japan, 2013.
- [20] G. Das, G. Mariotto, A. Quaranta, Microstructural evolution of thermally treated low-dielectric constant SiOC: H films prepared by PECVD, *J. Electrochem. Soc.* 153 (2006) F46–F51.
- [21] R.M. Almeida, C.G. Pantano, Structural investigation of silica gel films by infrared spectroscopy, *J. Appl. Phys.* 68 (1990) 4225–4232.
- [22] R. Riedel, I.-W. Chen, *Ceramic Science and Technology Volume 1 Structures*, Wiley-VCH, 2008.
- [23] A. Saha, R. Raj, Crystallization maps for SiOC amorphous ceramics, *J. Am. Ceram. Soc.* 90 (2007) 578–583.
- [24] A. Saha, R. Raj, D.L. Williamson, A model for the nanodomains in polymer-derived SiOC, *J. Am. Ceram. Soc.* 89 (2006) 2188–2195.
- [25] G. Mera, A. Navrotsky, S. Sen, H.-J. Kleebe, R. Riedel, Polymer-derived SiCN and SiOC ceramics – structure and energetics at the nanoscale, *J. Mater. Chem. A* 1 (2013) 3826–3836.
- [26] T. Yamaoka, K. Oyoshi, T. Tagami, Y. Arima, K. Yamashita, S. Tanaka, Crystallization of amorphous Si on a glass substrate through nucleation by Si^+ ion implantation, *Appl. Phys. Lett.* 57 (1990) 1970–1972.
- [27] V. Heera, R. Kögler, W. Skorupa, J. Stoemenos, Complete recrystallization of amorphous silicon carbide layers by ion irradiation, *Appl. Phys. Lett.* 67 (1995) 1999–2001.
- [28] S. Martínez-Crespiera, E. Ionescu, H.-J. Kleebe, R. Riedel, Pressureless synthesis of fully dense and crack-free SiOC bulk ceramics via photo-crosslinking and pyrolysis of a polysiloxane, *J. Eur. Ceram. Soc.* 31 (2011) 913–919.
- [29] C.G. Pantano, A.K. Singh, H. Zhang, Silicon oxycarbide glasses, *J. Sol-Gel Sci. Technol.* 25 (1999) 7–25.